

BabyAI 1.1

David Yu-Tung Hui¹, Maxime Chevalier-Boisvert¹, Dzmitry Bahdanau², and Yoshua Bengio^{1,3}

¹Mila, Université de Montréal

²Element AI

³CIFAR Senior Fellow

July 28, 2020

Abstract

The BabyAI platform is designed to measure the sample efficiency of training an agent to follow grounded-language instructions. BabyAI 1.0 presents baseline results of an agent trained by deep imitation or reinforcement learning. BabyAI 1.1 improves the agent’s architecture in three minor ways. This increases reinforcement learning sample efficiency by up to $3\times$ and improves imitation learning performance on the hardest level from 77% to 90.4%. We hope that these improvements increase the computational efficiency of BabyAI experiments and help users design better agents.

1 Introduction

The BabyAI platform ¹ is an environment designed to evaluate how well an agent follows grounded-language instructions. The quality of an agent is measured with two metrics: its success rate at following instructions and the number of episodes or demonstrations required to train it. BabyAI 1.0, [Chevalier-Boisvert et al., 2019], presents results of a baseline agent trained by reinforcement and imitation learning (RL and IL) methods. In this technical report, we present three modifications that significantly improved the baseline results.

Two modifications are to the network’s architecture and the third to the representation of the visual input. The network is modified by removing maxpooling at lower levels in the visual encoder and adding residual connections around FiLM layers [Perez et al., 2017]. The visual representation is modified to use learned embeddings in a Bag-of-Words fashion [Mikolov et al., 2013].

2 Proposed Architectural and Representational Modifications

This section describes the network architecture and BabyAI 1.0 visual representation before detailing the two architectural modifications and two alternate visual representations. The BabyAI platform has nineteen levels which can be categorised into two types: small and big [Chevalier-Boisvert et al., 2019]. Small levels are single-room but big levels are usually 3×3 rooms. The BabyAI 1.0 baseline agent has two architectures used on the small and big levels. These architectures have the same structure and are illustrated by Figure 1.a. The architecture takes two inputs, a visual input and a linguistic instruction. We use FiLM to combine the outputs of a convolutional ‘visual encoder’ with a GRU [Cho et al., 2014] embedding of the instruction. We refer the reader to Appendix A for more details concerning the distinction between ‘big’ and ‘small’.

Figures 1.b and 1.c respectively present two architectural modifications: removing pooling in the visual encoder and adding residual connections around the image convolution and the FiLM layers. To ensure that the shape of the visual encoder is consistent after pooling is removed, we change filter size from 2×2 to 3×3 . We expect these changes to improve sample efficiency because they enable more information to be transmitted to higher layers.

¹(<https://github.com/mila-iqia/babyai>)

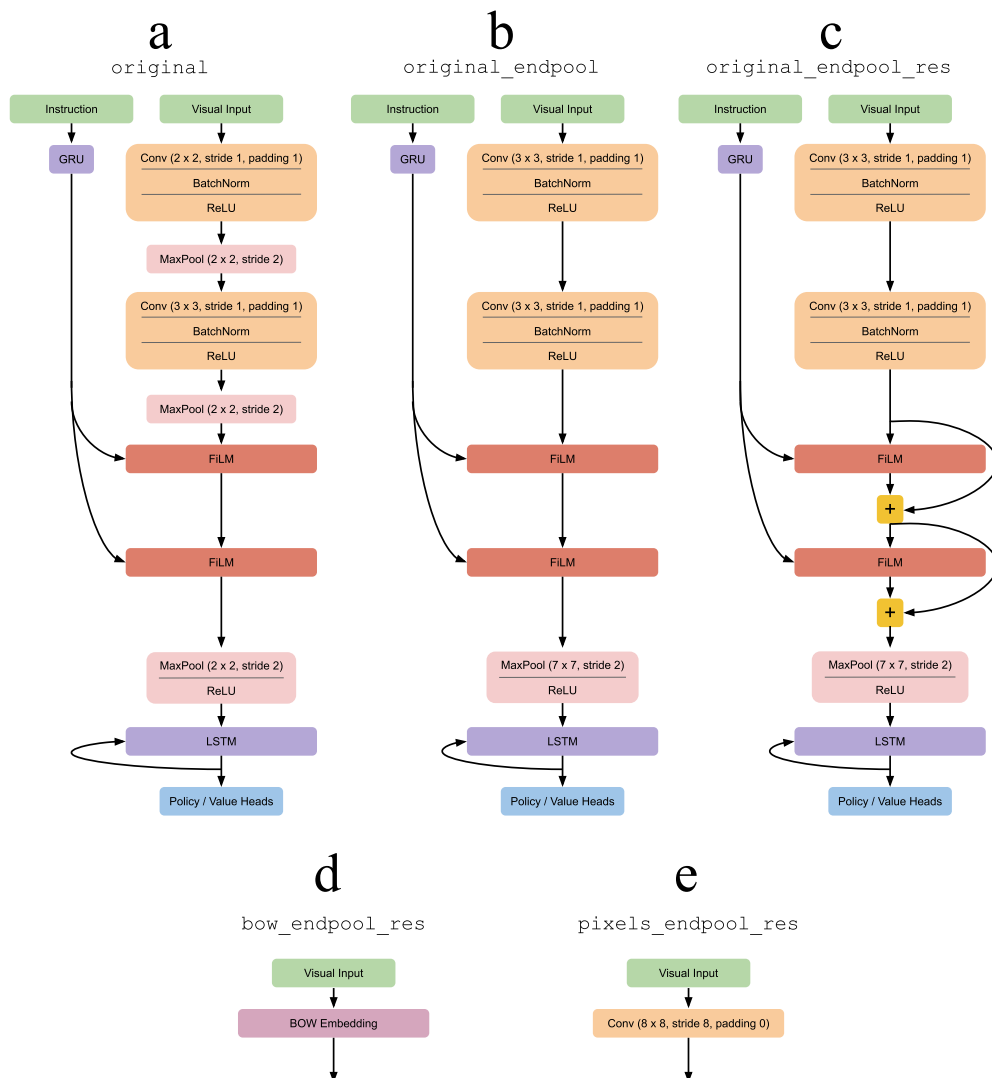


Figure 1: The five architectures. (a), (b) and (c): BabyAI 1.0 architecture, first modification removing pooling in the visual encoder and second modification introducing residual connections around FiLM. (d), (e): respective architectural changes needed to use BOW and pixel visual representations. Arrows at the bottom of architectures (d) and (e) feed into an architecture identical from the first convolutional layer of (c) onwards.

At every timestep, the agent receives visual information about a 7×7 grid of tiles which are immediately in the direction it is facing. BabyAI 1.0 represents a tile by a triple-integer value. The first integer describes the type of object in the tile and the second integer the object’s color. The third integer is only used if the object is a door, and describes whether it is open, closed or locked. BabyAI 1.0 represents a visual input by concatenating all tile representations together. This results in a tensor of size $7 \times 7 \times 3$.

A gridworld tile (and thus the visual input) can also be represented in two other ways: as a “bag of words” or by an RGB image. In the Bag-of-Words (“BOW”) approach a set of symbols that describes the tile is embedded in a trainable lookup table. This approach is commonly used in gridworlds such as [Leike et al., 2017], [Rajendran et al., 2015] and [Schrader, 2018]. Because a tile in BabyAI can be represented by three integers, we use three look-up tables and use each integer as a key. A tile is then represented by the mean of the three looked-up feature vectors. As with the BabyAI 1.0 visual representation, the BOW representation is formed from combining all tile representations into a 3D tensor. As we set the dimensionality of a feature vector to 128, the dimensionality of the BOW visual representation is $7 \times 7 \times 128$. This is depicted in Figure 1.d.

The contents of a tile can also be represented by a 3-channel Red-Green-Blue (RGB) image. As we choose the size of an image to be 8 pixels, a grid is thus represented by an image stored in a $8 \times 8 \times 3$ tensor. The entire 7×7 visual input can be represented in a 3-channel RGB image with dimensionality $56 \times 56 \times 3$. An architecture using this visual representation is illustrated in Figure 1.

Architecture names are structured in two parts. The first part is either “original”, “bow” or “pixels”, indicating which visual representation is used. The second part is optional and describes whether “_endpool” (because the only source of pooling is at the end) or “_res” (adding residual connections) are present in the architecture.

3 Experiments

To determine the best architecture and visual representation, we follow BabyAI 1.0 and experiment on the six easiest BabyAI levels. These six levels consist of five single-room levels and one multi-room level. Then, we present IL performance benchmarks on all levels.

3.1 Finding the Best Architecture

We measure RL sample and computational efficiency and IL performance with varying number of demonstrations. RL experiments were structured in two stages.

The first set of experiments investigated architectural modifications. Results in Table 1a showed that removing pooling in the visual encoder had a significant improvement on sample efficiency, but adding residual connections effected both increases and decreases. Nevertheless, we adopted residual connections for further experiments because the sample efficiency increase for PutNextLocal greatly outweighed the total decrease in GoToLocal and GoTo.

The second set of experiments investigated visual representations. Results in Table 1b still do not show a wide variation in sample efficiency. Because training from pixels was hard on the two most difficult levels (GoTo, PutNextLocal), we halved the learning rate (α in Adam [Kingma and Ba, 2015]) from 1×10^{-4} to 5×10^{-5} and reran the second set of experiments. The resulting statistics in Table 1c do not show much variation between the three visual representations.

We now consider the computational efficiency of training each of these five architectures. Training from pixels has a slower throughput than the other visual representations (Table 2). Because of this and no clear advantage in RL sample efficiency (Tables 1b, 1c), we drop further experiments on pixels.

Now, we investigate whether changing the visual representation to BOW and two architectural modifications improve IL performance. Chevalier-Boisvert et al. [2019] measures sample efficiency using an interpolated function fitted with a Gaussian Process (GP) [Rasmussen and Williams, 2005]. In our experiments we found that an infeasibly large number of training runs would be required in order to obtain a sufficiently confident sample efficiency estimate from the GP. Instead, we follow Table 6 in [Żoła et al., 2020], who evaluate IL by observing its success rate trained with varying number of demonstrations. Żoła et al. [2020] use $1/64^{\text{th}}$, $1/8^{\text{th}}$ and all of 1 million demonstrations. We use 5, 10, 50, 100 and 500 thousand demonstrations, which correspond to $1/200^{\text{th}}$, $1/100^{\text{th}}$, $1/20^{\text{th}}$, $1/10^{\text{th}}$ and $1/2^{\text{th}}$ of the total 1 million demonstrations.

IL results in Table 3 show that training from BOW is advantageous to the original BabyAI 1.0 visual representation. Interestingly, we find that for hard levels with a few number of demos, the architectural modifications are not beneficial for training. This is offset by changing the visual representation to BOW.

3.2 Benchmarking the Best Modifications

Having constructed the BabyAI 1.1 agent, we benchmark its performance over all nineteen BabyAI levels.

Table 4 shows that modifications found by the previous section yielded improvements in performance over all levels. Four more levels (Unlock, Putnext, Synth and SynthLoc) were solved, and success rate increased by 13.7% in the hardest level (BossLevel) from 77% to 90.4%.

4 Conclusion

As BabyAI was intended to be a lightweight experimental platform, BabyAI 1.0 used a specific hand-crafted representation rather than a more realistic pixel-based representation. We have shown that training from other visual representations (BOW and pixels) is feasible, and is sometimes more sample efficient (Table 3). However, learning from pixels took longer to compute (Table 2) and was more sensitive to hyperparameters. Besides, using pixel representations for the tiles still does not bridge the reality gap between the gridworld and the 3D real world, for almost all challenging aspects of visual perception, such as e.g. occlusion, illumination, different viewpoints are still not modelled. For this reason we keep the BabyAI input representation symbolic, though we switch to the more standard BOW approach for encoding the symbolic input.

This report introduces BabyAI 1.1, the latest version of the BabyAI platform. This modifies the previous version of BabyAI with minor changes to the baseline agent, but major improvements to baseline statistics. We hope that this change encourages researchers to (re-)use similar architectures within novel agents, so that research into grounded language learning may be conducted in more computationally efficient ways.

Acknowledgements

This research was mostly performed at Mila with funding by the Government of Quebec and CIFAR, and enabled by Compute Canada (www.computecanada.ca).

Table 1: RL sample efficiency (mean \pm std, thousands of episodes) in the six easiest BabyAI levels with respect to different *architectures* (Table 1a) and *visual representations* with $1e-4$ learning rate (Table 1b) and $5e-5$ learning rate (Table 1c). Each figure is an average over ten training runs initialised to a randomly chosen seed. All experiments were run with the ‘small’ architecture. More experimental details are in Appendix B.

A cell is shaded depending on whether its values are statistically significant from those of the cell *to its left*. Statistical significance is computed using a two-tailed T-test with unequal variance.

accept null hypothesis that there is *no significant difference*

reject null hypothesis at 1 % significance due to *significant increase in sample efficiency* (number is smaller)

reject null hypothesis at 1 % significance due to *significant decrease in sample efficiency* (number is bigger)

(a) RL sample efficiency for different architectures. See the last paragraph of Section 2 for the explanation of architecture names.

Level	Sample Efficiency		
	original	original_endpool	original_endpool_res
GoToRedBallGrey	21 \pm 5	21 \pm 6	21 \pm 5
GoToRedBall	273 \pm 27	200 \pm 16	179 \pm 17
GoToLocal	1311 \pm 251	381 \pm 30	437 \pm 45
PickupLoc	1797 \pm 290	743 \pm 132	710 \pm 166
PutNextLocal	2984 \pm 172	2169 \pm 739	1009 \pm 128
GoTo	1601 \pm 463	454 \pm 69	813 \pm 278

(b) RL sample efficiency for different visual representations with $learning\ rate = 10^{-4}$. See the last paragraph of Section 2 for the explanation of architecture names.

Level	Sample Efficiency		
	original_endpool_res	bow_endpool_res	pixels_endpool_res
GoToRedBallGrey	21 \pm 5	24 \pm 2	34 \pm 4
GoToRedBall	179 \pm 17	177 \pm 2	172 \pm 2
GoToLocal	437 \pm 45	611 \pm 760	242 \pm 15
PickupLoc	710 \pm 166	982 \pm 266	1082 \pm 385
PutNextLocal	1092 \pm 143	876 \pm 104	Not Trainable
GoTo	813 \pm 278	817 \pm 502	Not Trainable

(c) RL sample efficiency for different visual representations with $learning\ rate = 5 \times 10^{-5}$. See the last paragraph of Section 2 for the explanation of architecture names.

Level	Sample Efficiency		
	original_endpool_res	bow_endpool_res	pixels_endpool_res
GoToRedBallGrey	35 \pm 5	30 \pm 4	44 \pm 11
GoToRedBall	263 \pm 22	164 \pm 3	155 \pm 5
GoToLocal	606 \pm 81	449 \pm 176	336 \pm 28
PickupLoc	1732 \pm 579	1461 \pm 422	1308 \pm 421
PutNextLocal	1277 \pm 252	876 \pm 104	1301 \pm 320
GoTo	984 \pm 484	803 \pm 525	845 \pm 329

Table 2: Frames Per Second (mean \pm std) of RL training with different architectures, averaged across the six easiest BabyAI levels. Inter-level differences are negligible.

Architecture	original	original_endpool	original_endpool_res	bow_endpool_res	pixels_endpool_res
RL (FPS)	1139 \pm 128	927 \pm 72	907 \pm 69	855 \pm 58	540 \pm 67

Table 3: IL success rate (%) in the six easiest BabyAI levels with respect to varying number of demonstrations, architectures and visual representations. Experiments have a success rate $\geq 99\%$ are successful and are **bolded**. Each figure is an average over ten training runs initialised to a randomly chosen seed. Standard deviations of ± 0.0 are omitted for clarity. The first five experiments were run with the ‘small’ architecture. GoTo experiments were run with the ‘large’ architecture. More experimental details are given in Appendix C.

A cell is shaded depending on whether its values are statistically significant from those of the cell *to its left*. Statistical significance is computed using a two-tailed T-test with unequal variance.

- accept null hypothesis that there is *no significant difference*
- reject null hypothesis at 1 % significance due to *significant increase in performance* (number is bigger)
- reject null hypothesis at 1 % significance due to *significant decrease in performance* (number is smaller)

Level	Number of Demos (thousands)	Success Rate		
		original	original_endpool_res	bow_endpool_res
GoToRedBallGrey	5	99.5 \pm 0.1	99.5 \pm 0.1	99.7 \pm 0.1
	10	99.7	99.8 \pm 0.1	99.9
	50	100	100	100
	100	100	100	100
	500	100	100	100
GoToRedBall	5	89.6 \pm 0.3	91.3 \pm 0.6	99.3 \pm 0.3
	10	93.1 \pm 0.8	95.6 \pm 0.7	99.8 \pm 0.1
	50	99.2 \pm 0.2	99.9	100
	100	99.7	100	100
	500	99.9	100	100
GoToLocal	5	72.5 \pm 1.0	71.6 \pm 1.4	84.2 \pm 2.0
	10	79.9 \pm 1.2	79.7 \pm 1.8	94.2 \pm 0.8
	50	95.3 \pm 0.5	99.6 \pm 0.1	99.8 \pm 0.1
	100	97.8 \pm 0.3	99.9	99.9
	500	99.6 \pm 0.1	100	100
PutNextLocal	5	22.3 \pm 1.7	12.0 \pm 1.8	12.5 \pm 1.2
	10	39.1 \pm 3.5	16.2 \pm 2.3	24.9 \pm 3.2
	50	80.8 \pm 1.4	90.6 \pm 3.5	88.6 \pm 11.0
	100	93.9 \pm 0.4	99.5 \pm 0.1	99.5 \pm 0.5
	500	99.3 \pm 0.2	100	100
PickupLoc	5	53.0 \pm 1.3	35.9 \pm 1.5	60.3 \pm 1.8
	10	65.3 \pm 1.5	53.7 \pm 1.2	74.9 \pm 3.9
	50	90.8 \pm 1.5	96.2 \pm 0.5	97.0 \pm 0.3
	100	96.4 \pm 0.5	98.5 \pm 0.4	98.6 \pm 0.3
	500	99.5 \pm 0.2	99.8 \pm 0.1	99.8 \pm 0.1
GoTo	10	70.4 \pm 1.1	76.3 \pm 5.0	96.1 \pm 0.4
	100	94.9 \pm 0.3	99.3 \pm 0.1	99.4

Table 4: Comparison of baseline IL results for all BabyAI levels. Experiments with a success rate $\geq 99\%$ are successful and are **bolded**. On all levels, the ‘big’ configuration was trained on 1 million demonstrations until the loss has converged. As running these experiments are computationally expensive, we present results on 1 seed. Success rate is calculated as with 512 trials once the loss has converged.

Level	Success Rate (%)		Demo Length (Mean \pm Std)
	BabyAI 1.0	BabyAI 1.1	
GoToObj	100	100	5.18 \pm 2.38
GoToRedBallGrey	100	100	5.81 \pm 3.29
GoToRedBall	100	100	5.38 \pm 3.13
GoToLocal	99.8	100	5.04 \pm 2.76
PutNextLocal	99.2	100	12.4 \pm 4.54
PickupLoc	99.4	100	6.13 \pm 2.97
GoToObjMaze	99.9	100	70.8 \pm 48.9
GoTo	99.4	100	56.8 \pm 46.7
Pickup	99	100	57.8 \pm 46.7
UnblockPickup	99	100	57.2 \pm 50
Open	100	100	31.5 \pm 30.5
Unlock	98.4	100	81.6 \pm 61.1
PutNext	98.8	99.6	89.9 \pm 49.6
Synth	97.3	100	50.4 \pm 49.3
SynthLoc	97.9	100	47.9 \pm 47.9
GoToSeq	95.4	96.7	72.7 \pm 52.2
SynthSeq	87.7	93.9	81.8 \pm 61.3
GoToImpUnlock	87.2	84.0	110 \pm 81.9
BossLevel	77	90.4	84.3 \pm 64.5

References

- Bahdanau, D., Cho, K., and Bengio, Y. (2015). Neural Machine Translation by Jointly Learning to Align and Translate. In *Proceedings of the 2015 International Conference on Learning Representations*.
- Chevalier-Boisvert, M., Bahdanau, D., Lahlou, S., Willems, L., Saharia, C., Nguyen, T. H., and Bengio, Y. (2019). BabyAI: First steps towards grounded language learning with a human in the loop. In *International Conference on Learning Representations*.
- Cho, K., van Merriënboer, B., Gulcehre, C., Bougares, F., Schwenk, H., and Bengio, Y. (2014). Learning Phrase Representations using RNN Encoder-Decoder for Statistical Machine Translation. In *Proceedings of the 2014 Conference on Empirical Methods in Natural Language Processing (EMNLP)*.
- Hochreiter, S. and Schmidhuber, J. (1997). Long Short-Term Memory. *Neural Computation*, 9(8):1735–1780.
- Kingma, D. P. and Ba, J. (2015). Adam: A Method for Stochastic Optimization. In *Proceedings of the 2015 International Conference on Learning Representations*. arXiv: 1412.6980.
- Leike, J., Martic, M., Krakovna, V., Ortega, P. A., Everitt, T., Lefrancq, A., Orseau, L., and Legg, S. (2017). Ai safety gridworlds. *arXiv preprint arXiv:1711.09883*.
- Mikolov, T., Chen, K., Corrado, G., and Dean, J. (2013). Efficient estimation of word representations in vector space. *arXiv preprint arXiv:1301.3781*.
- Perez, E., Strub, F., de Vries, H., Dumoulin, V., and Courville, A. (2017). FiLM: Visual Reasoning with a General Conditioning Layer. In *Proceedings of the 2017 AAAI Conference on Artificial Intelligence*.
- Rajendran, J., Lakshminarayanan, A. S., Khapra, M. M., Prasanna, P., and Ravindran, B. (2015). Attend, adapt and transfer: Attentive deep architecture for adaptive transfer from multiple sources in the same domain. In *Proceedings of the 2017 International Conference on Learning Representations*.
- Rasmussen, C. E. and Williams, C. K. I. (2005). Gaussian Processes for Machine Learning. In *Adaptive Computation and Machine Learning*.
- Schrader, M.-P. B. (2018). gym-sokoban. <https://github.com/mpSchrader/gym-sokoban>.
- Schulman, J., Moritz, P., Levine, S., Jordan, M., and Abbeel, P. (2015). High-Dimensional Continuous Control Using Generalized Advantage Estimation. In *Advances in Neural Information Processing Systems 30*.
- Schulman, J., Wolski, F., Dhariwal, P., Radford, A., and Klimov, O. (2017). Proximal Policy Optimization Algorithms. *arXiv:1707.06347 [cs]*. arXiv: 1707.06347.
- Werbos, P. J. (1990). Backpropagation through time: what it does and how to do it. *Proceedings of the IEEE*, 78(10):1550–1560.
- Wu, Y., Mansimov, E., Liao, S., Grosse, R. B., and Ba, J. (2017). Scalable trust-region method for deep reinforcement learning using kronecker-factored approximation. *CoRR*, abs/1708.05144.
- Żoła, K., Saharia, C., Boussioux, L., Hui, D. Y.-T., Chevalier-Boisvert, M., Bahdanau, D., and Bengio, Y. (2020). Combating false negatives in adversarial imitation learning. *arXiv preprint arXiv:2002.00412*.

A Agent Architecture

At every timestep, an agent receives a visual input and linguistic command of variable length which compels the agent to execute an action. The BabyAI baseline agent is implemented by a deep neural network which processes the visual input and linguistic command, producing an action. The visual input and linguistic instruction are respectively encoded by a Gated Recurrent Unit (GRU) and convolutional network. These two encodings are then combined by two batch-normalised FiLM layers. A Long-Short-Term-Memory cell (LSTM) [Hochreiter and Schmidhuber, 1997] integrates the output of FiLM across timesteps. Finally, the integrated output is passed to policy and value heads.

The agent can be trained by RL or IL methods in conjunction with BackPropagation Through Time (BPTT) [Werbos, 1990].

The ‘small’ configuration uses a unidirectional GRU and LSTM of dimensionality 128 for memory. The ‘big’ configuration uses a 128-dimensional bidirectional GRU with attention [Bahdanau et al., 2015] and the memory LSTM with dimensionality 2048.

B Reinforcement Learning Experiments

Sample efficiency is defined by the number of RL training episodes needed to train an agent to $\geq 99\%$ success rate. Chevalier-Boisvert et al. [2019] defines success as whether an agent can follow an instruction within n_{max} steps, a figure pre-defined for each level.

We use Advantage-Actor Critic (A2C) [Wu et al., 2017] with Proximal Policy Optimisation (PPO) [Schulman et al., 2017] and Generalised Advantage Estimation (GAE) [Schulman et al., 2015]. Data for A2C is collected in batches of 64 rollouts of length 40. These were used in 4 epochs of PPO. $\lambda = 0.99$ was used in GAE. If an agent completes a task after n steps, it is rewarded with $1 - 0.9n/n_{max}$. Otherwise, no reward is given. The returns were discounted by $\gamma = 0.99$. Results in Table 1a and Table 1b was optimised by Adam with the hyperparameters $\alpha = 10^{-4}$, $\beta_1 = 0.9$, $\beta_2 = 0.999$ and $\epsilon = 10^{-5}$. Results in Table 1c used $\alpha = 5 \times 10^{-5}$.

C Imitation Learning Experiments

Different hyperparameters were used for training ‘small’ and ‘big’ models.

The small model was trained with a batch size of 256 and an epoch consisting of 25600 demos. Backpropagation Through Time (BPTT) was truncated at 20 steps.

The large model had a batch size of 128 and an epoch of 102400 demonstrations. BPTT was truncated at 80 steps. In addition, the model was trained with an entropy regulariser, which had a coefficient of 0.01.

These were optimised by Adam with $\alpha = 10^{-4}$ for small architectures, $\alpha = 5 \times 10^{-5}$ for large architectures and $\beta_1 = 0.9$, $\beta_2 = 0.999$ and $\epsilon = 10^{-5}$.